

Structural analysis of nano-sized-Pd/ZrO₂ composite after H(D) absorption

Yoshinori Arachi^{a,*}, Shuichi Emura^b, Akira Omura^c, Masanobu Nunogaki^b, Takeshi Asai^a,
Shunichi Yamaura^d, Akihisa Inoue^d, Yoshiaki Arata^c

^a Faculty of Engineering, Kansai University, Suita, Osaka 564-8680, Japan

^b ISIR, Osaka University, Mihogaoka 8-1, Ibaraki, Osaka 567-0047, Japan

^c Academician, Osaka University, Yamadaoka 2-1, Suita, Osaka 567-0871, Japan

^d Institute for Materials Research, Tohoku University, Sendai, Miyagi 980-8577, Japan

Received 11 July 2005; received in revised form 10 April 2006; accepted 10 April 2006

Abstract

Structural analysis of high density H(D) absorbed Pd particles with 5 nm dispersed ZrO₂ has been carried out using XAFS (X-ray Absorption Fine Structure) techniques. X-ray absorption spectra around the Pd *K*-absorption edge were observed and analyzed. The Pd–Pd bonding distance was enlarged by 0.08 Å during absorption of deuterium, and it completely reverted to its original state with the release of deuterium while maintaining the crystal lattice symmetry. These changes provide evidence that deuterium locates not on the surface of the Pd particle, but rather within the Pd crystal lattice. The hydrogen absorption mechanism will also be discussed.

© 2006 Elsevier B.V. All rights reserved.

Keywords: Hydrogen absorption; XAFS; Nano-sized composite

1. Introduction

Hydrogen storage materials play an important role in power portable electronic devices that use fuel cells. In the search for new materials, nanostructured materials sometimes yield anomalous effects due to their unique nanometer-scale structure. The nanocomposite material consisting of Pd and ZrO₂ is one such material [1,2,3]. Studies on hydrogen absorption of nanoscale Pd particles have been investigated experimentally and theoretically [3–11]. Eastman et al. have described the differences in the hydrogenation behavior of coarse-grained bulk Pd and nanocrystalline Pd [4]. The hydrogen solubility increased with decreasing grain size, and Pd nanocrystals had a smaller miscibility gap than the Pd bulk. They suggested that the hydrogen absorption properties strongly depend on the surface characteristics of the particles. S. Yamaura et al. have reported hydrogen absorption of nanoscale Pd particles embedded in ZrO₂ [3]. This material absorbs 2.4 mass% (H₂/Pd) of hydrogen at 323 K and 2.2 mass% (H₂/Pd) of hydrogen at 423 K at an

applied hydrogen pressure of 1 MPa. Oxidizing Zr₆₅Pd₃₅ alloy in air leads to the synthesis of nano-sized Pd particles in ZrO₂ with PdO, which means that the PdO is formed in addition to the Pd particles within the ZrO₂ matrix. Y. Arata and Y.C. Zhang have reduced PdO in ZrO₂ by an appropriate method and obtained pure Pd particles with 5 nm or smaller size, embedded and dispersed in ZrO₂ powder. In addition, they were able to significantly improve hydrogen absorption performance, forming high density hydrogen lumps in Pd [1,2]. However, there is very little information available on the absorption process, specifically about the structure of the Pd itself that affects hydrogen absorption. X-ray and neutron diffraction patterns indicated no contribution of Pd particles towards hydrogen absorption because of their extremely small size. We have already confirmed that a specific amount of deuterium atoms per unit Pd cell are absorbed, and that the ZrO₂ powder is inactive for absorbing hydrogen. Moreover, the absorption proceeds through an exothermic process and is reversible [1,2].

In the present study, in order to elucidate the absorption process, we have adopted the XAFS technique which is a very powerful tool for observing structural changes with short range

* Corresponding author.

E-mail address: arachi@ipcku.kansai-u.ac.jp (Y. Arachi).

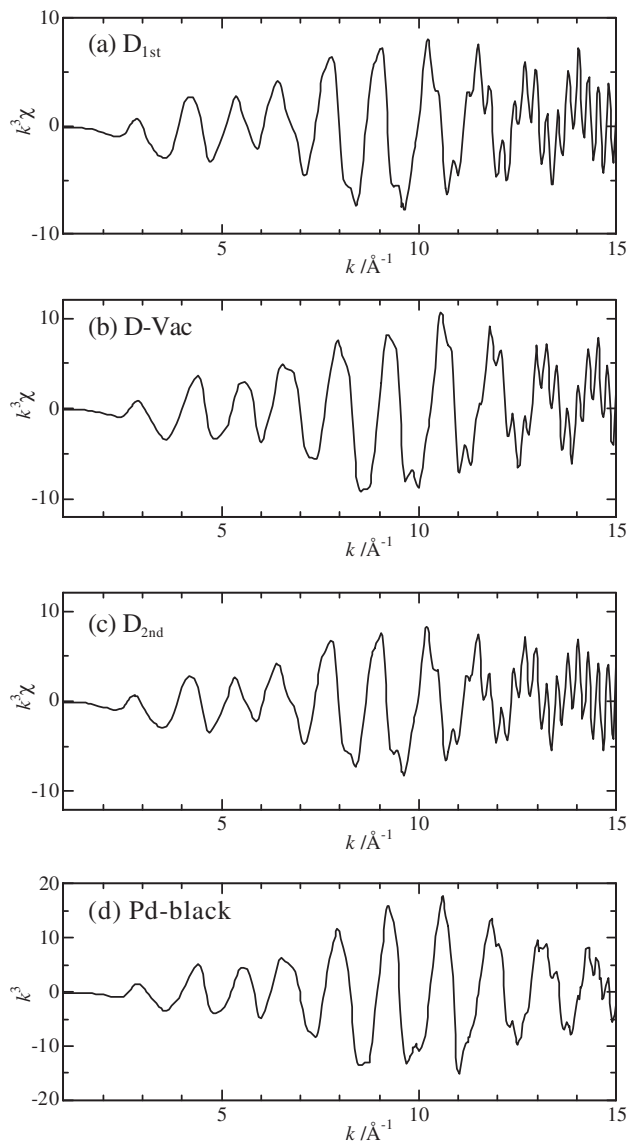


Fig. 1. Pd K -edge EXAFS oscillation function $k^3\chi(k)$ for (a) D_{1st} , (b) $D\text{-Vac}$, (c) D_{2nd} and (d) Pd-black.

order. As deuterium atoms are too light to detect XAFS signals, we take an indirect path to examine the Pd–Pd distance instead of the direct Pd–D/H distance.

2. Experimental

Nano-sized-Pd (5 nm^ϕ)/ZrO₂ composites were examined in this study. Zr₆₅Pd₃₅ was prepared from a mixture of pure Zr and Pd metals by melting in an Ar atmosphere, and Pd particles embedded in ZrO₂ were obtained by oxidizing the amorphous Zr₆₅Pd₃₅ alloy at 553 K for 24 h in air. To obtain the nano-sized-Pd/ZrO₂ composite, the above Pd particles embedded in ZrO₂ were baked at 423 K for 48 h in vacuum (10^{−7} Torr). Details of the preparation of these nanocomposite materials are described in Refs. [1,2]. The as-prepared nano-sized-Pd/ZrO₂ composites were treated for XAFS measurements as follows. First, they were introduced into a quartz vessel with a gap of 50–100 μm and thickness of 0.5 mm with the assistance of supersonic

waves. To remove some of the adsorbed atoms or ions, the material in the vessel was kept in a vacuum of 8×10^{-7} Torr at about 400 K for 24 h (denoted as Vac hereafter). D₂ gas was injected into Vac at 0.2 MPa at room temperature (D_{1st}) and then the vessel was evacuated to 8×10^{-7} Torr at 400 K ($D\text{-Vac}$). Finally D₂ gas was again injected into the vessel at 0.2 MPa at room temperature (D_{2nd}).

X-ray absorption spectra of the Pd K -edge using synchrotron radiation were measured at BL19B2 (SPring-8) and BL10B (PF) in a transmission mode at 295 K. The X-rays were monochromatized by a Si(111) double crystal. Incident and transmitted X-rays are detected by ion chambers filled with 50% Ar and 50% N₂ gases, and 100% Ar gas, respectively. Glass with a total thickness of 1 mm reduced the incident X-rays to about half at the Pd K -edge threshold energy (24.35 keV). The Pd K -edge data were analyzed using the Rigaku REX2000 code. Backgrounds were subtracted from the pre-edge region using an extrapolated Victoreen-plus-constant type function, and the XAFS oscillations $\chi(k)$ were extracted using cubic spline baseline functions. Fourier transforms were performed on the normalized $\chi(k)$ with k^3 weighting of a Hanning window in the region $k=1.2\text{--}15.0 \text{ \AA}^{-1}$. Curve-fitting was carried out using a single shell model in the range filtered from 1.6 to 3.1 Å in R for Pd–Pd. The coordination numbers were initially fixed at 12 and then analyzed as changeable parameters.

3. Results and discussion

XRD patterns for Zr₆₅Pd₃₅ oxidized at 553 K for 24 h showed mixed phases consisting of monoclinic and cubic ZrO₂. No clear peaks corresponding to Pd particles were observed because of their extremely small size. Using scanning electron microscopy (SEM), the particle size of the dispersed Pd in ZrO₂ was measured to be about 5 nm. The characteristics of D₂/H₂

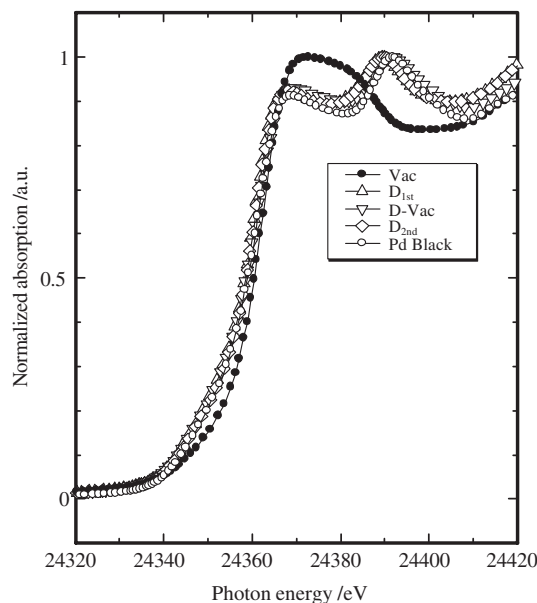


Fig. 2. XANES spectra of Pd K -edge for the D_{1st} , $D\text{-Vac}$, D_{2nd} and Pd-black nano-sized-Pd/ZrO₂ composites.

absorption into the nano-sized-Pd/ZrO₂ composite as well as the microstructure have been described in Refs. [1–3].

Figs. 1 and 2 show normalized X-ray absorption spectra and the XANES region around the Pd *K*-edge threshold, respectively, for the nano-sized-Pd/ZrO₂ composite specimens, D_{1st}, D-Vac, D_{2nd} and Pd-black. Commercial Pd-black was used as a reference and is included in these figures for comparison. An obvious change in the period of XAFS oscillations between the deuterium-injected specimen (D_{1st}) and the deuterium-removed specimen (D-Vac) is observed. The period of XAFS oscillations of a Pd-black (bulk specimen) is almost the same as for the D-Vac specimen. This suggests that the environment of any Pd atom in the D-Vac specimen returns to its original state by removing deuterium. The insignificant difference in the XANES spectra among D_{1st}, D-Vac, D_{2nd} and Pd-black specimens indicates that the electron valency of Pd in all the specimens is the same. By Fourier transforming the extracted XAFS oscillations (denoted by χ hereafter), the radial distribution functions (RDF) around the Pd atom are obtained, as shown in Fig. 3. The first main peak around 2.4 Å corresponds to the first neighbors. Here, it should be noted that the peak value in the RDF is not the exact bonding distance, and the precise Pd–Pd bonding distance can be obtained by correcting the phase shifts on emitting and scattering. The peak clearly shifts to a shorter distance by subjecting the D_{1st} specimen to vacuum, and the D_{2nd} specimen with deuterium re-injected returns to the elongated state for the bonding distance. It is evident that the RDFs of both the D_{1st} and D_{2nd} specimens overlap fairly over a wide range of *r*, yielding surprising reproducibility. The decrease in bonding distance can be attributed to an alteration in the Pd lattice. Injecting D₂ into the nano-sized-Pd/ZrO₂ composite causes lattice expansion, and this alteration is reversible. We have already confirmed that a specific amount of deuterium atoms per unit Pd cell is absorbed through an exothermic process by injecting D₂ and this absorption process is reversible [1,2]. Therefore, it can be concluded that the observed change in RDF reflects the absorption process.

Curve-fitting and quantitative analysis were carried out mainly for the first neighbor of Pd, based on the crystal structure

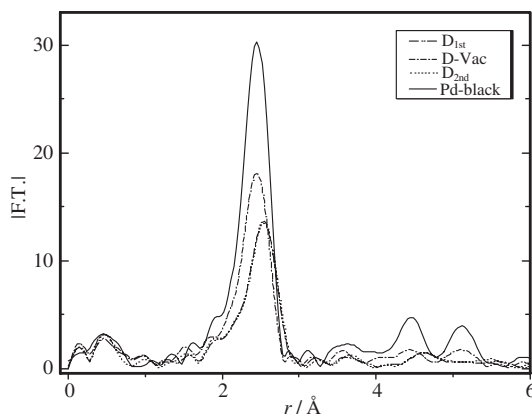


Fig. 3. Radial distribution functions (RDF) for the D_{1st}, D-Vac, D_{2nd} and Pd-black nano-sized-Pd/ZrO₂ composites.

Table 1

Structure parameters for the nano-sized-Pd/ZrO₂ composites obtained from the curve-fitting using one shell (Pd–Pd)

	<i>d</i> (Pd–Pd)/Å	$\sigma/\text{Å}^2$	<i>R</i> /%
D _{1st}	2.82	0.081	1.79
D-Vac	2.73	0.075	1.28
D _{2nd}	2.82	0.082	2.02
Pd-black	2.74	0.069	1.29

The *R* range used is from 1.83 to 3.03 Å: *d*=Pd–Pd distance, σ =the Debye–Waller factor, $R(\%) = \frac{\sum \{k^3 \chi_{\text{obs}} - k^3 \chi_{\text{cal}}\}^2}{\sum \{k^3 \chi_{\text{obs}}\}^2}$.

of the Pd metal [12]. The results of various states are summarized in Table 1. We initially assumed that the first neighbors of Pd for all specimens are only Pd, and it is coordinated with 12 Pd atoms. Hence, the first peak shown in Fig. 3 corresponds to a Pd–Pd single shell. The coordination number is initially fixed at 12 and is then analyzed as a changeable parameter. However, no significant change was detected in the results obtained for both conditions. The estimated standard deviation (*R* factor) for all shows enough low to discuss. The fitting quality of D-Vac as an example is demonstrated in Fig. 4, showing the inverse Fourier transformation around 2.4 Å in RDF. The structural parameters for D-Vac are similar to that of Pd-black which is used as a reference. The Pd–Pd bonding distance changes by 0.08 Å with deuterium being absorbed and desorbed, as observed in the change in RDF. Since the parameters for D_{1st} are the same as those for D_{2nd}, it was proved that the structure returned to the original state and proceeded while maintaining the lattice symmetry. This is obvious evidence to indicate local structural change in hydrogen absorbing materials.

Generally, for interstitial hydrides, there are the following possibilities for hydrogen to locate in the Pd/M (M: metal) lattice with the face centered cubic structure (fcc) [13,14]. Fitting hydrogen atoms into octahedral or tetrahedral holes in the metal lattice, or a combination of the two allows the structure limit to have compositions of MH, MH₂, and MH₃. The Pd–Pd bonding distance for D_{1st} obtained is shown in Table 1 and for interstitial octahedral and tetrahedral spaces is 1.18 Å for octahedral and 0.64 Å for tetrahedral, respectively. Due to the hydrogen radius, it is likely for hydrogen to locate in the

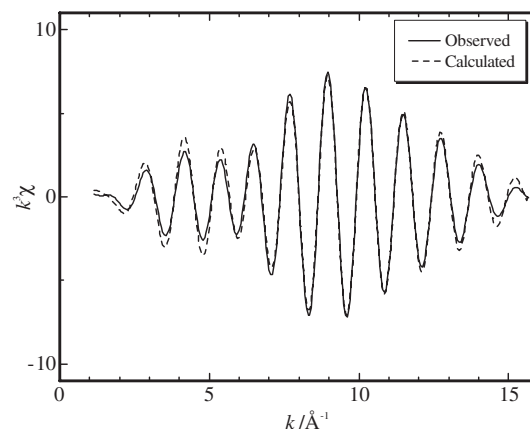


Fig. 4. Representative curve-fitting results using the Pd–Pd one shell model for D-Vac as an example.

former site. The secondary H/Pd system is well established [15]. For a small hydrogen-to-metal ratio ($H/M < 0.1$), the hydrogen is exothermically dissolved in the metal and the metal lattice expands proportional to the hydrogen concentration. At greater hydrogen concentrations in the host metal ($H/M > 0.1$), a strong hydrogen–hydrogen interaction may become important, and the hydride phase may nucleate and grow [16]. However, we have little information about where deuterium atoms are located in the nano-sized-Pd/ZrO₂ composites. It is well known that the hydrogen carries a partial positive charge and Pd is an extremely good hydrogenation catalyst [17]. That is because there is the possibility for protons to conduct as well. Further investigations are planned to clarify these issues.

Next, we inspect the Arata model [1] of the deuterium position and its arrangement. We already know that the exothermic process suggests 16 deuterium atoms per Pd fcc unit cell, that is 4 deuterium atoms per one Pd atom, are absorbed for the specimen in the saturated state. Four deuterium atoms are located in the octahedral space in the Pd fcc lattice toward tetrahedral ($\langle 111 \rangle$ and its equivalent) directions. The gap at the center of the octahedral point is 1.13 Å along the $\langle 100 \rangle$ axis and 3.96 Å along the $\langle 111 \rangle$ axis in the rigid shell model, after the Arata model. Since the octahedral space is sufficiently large to locate one deuterium atom, the deuterium atom loosely occupies this space. In such a case, central lattice instability is widely known as in super ionic conductors. The deuterium atom at a true octahedral center shifts by a small distance depending on the strength of the electron–lattice interaction in the $\langle 111 \rangle$ direction or its equivalent. The electron–lattice interaction is an inverse $\langle \varphi_p(\mathbf{r}) | (\partial V(\mathbf{r}, \mathbf{Q}_{T1u}) / \partial \mathbf{Q}_{T1u}) | \varphi_s(\mathbf{r}) \rangle \mathbf{Q}_{T1u}$ type in this case [18–20], and induces eight equivalent potential minimums along $\langle 111 \rangle$ and its equivalent directions away from the center. Four of these should be occupied by deuterium atoms in the tetrahedral alignment. It is difficult for such a high density of protons to exist because of the strong repulsion force between the protons. Moreover, as the proton is a Fermi particle, the energy level of proton must be placed by only two protons with anti-parallel spin. Thus, two protons of the four must occupy higher energy levels. However, in such cases, exchange interactions between protons allow the energy level to be lower. Furthermore, deuterium is composed of one proton and one neutron with anti-parallel spins, that is, deuterium is a Bose particle. Therefore, it seems to be possible for a highly dense state of protons to occupy the octahedral space. We consider that Pd in the initially prepared materials (pre-treated materials supplied for XAFS measurements) is in a partially oxidized state. That is, the materials are composed of nano-sized Pd, nano-sized PdO and ZrO₂. A XANES spectrum around the Pd *K*-edge for as-prepared specimens (Vac) shows a clear oxidized state. XAFS analysis gives the distance between Pd and O to be somewhat different from that of bulk PdO. Further results will appear in a following paper.

4. Summary

X-ray absorption spectra around the Pd *K*-absorption edge are observed and analyzed. The Pd–Pd bonding distance elongates by 0.08 Å through the absorption of deuterium atoms. The elongation is uniform and isotropic within the analysis limitations of the XAFS method. These changes provide evidence that deuterium does not locate on the surface of a Pd particle, but rather within the Pd crystal lattice. In addition, the expansion proceeds while maintaining the Pd lattice (fcc) symmetry and is reversible. Possible positions of the absorbed deuterium are octahedral interstitial locations in the Pd metal unit cell. This supports the Arata model proposed in Ref. [1]. The initially prepared nano-composite materials partially contain PdO. However, the Pd–O distance in the initial specimen is different from that of bulk PdO.

Acknowledgements

One of authors (S.E) greatly appreciates Academician H. Fujita for discussions on the structure analysis. The XAFS measurements were performed at SPring-8 in cooperation with the Japan Synchrotron Radiation Research Institute (JASRI) through Proposal No. 2004A0549-NI-np, and in part, at PF through Proposal No. 2004G065.

References

- [1] Y. Arata, Y.C. Zhang, Proc. Jpn. Acad. 78 (2002) 57.
- [2] Y. Arata, Y.C. Zhang, J. High Temp. Soc. 29 (2003) 1.
- [3] S. Yamaura, K. Sasamori, H. Kimura, A. Inoue, J. Mater. Res. 17 (2002) 1329.
- [4] J.A. Eastman, L.J. Thompson, B.J. Kestel, Phys. Rev., B 48 (1993) 84.
- [5] A. Züttel, Ch. Nützenadel, G. Schmid, D. Chartouni, L. Schlapbach, J. Alloys Compd. 293–295 (1999) 472.
- [6] W.C. Chen, Brent J. Heuser, J. Alloys Compd. 312 (2000) 176.
- [7] T. Yokoyama, T. Ohta, Jpn. J. Appl. Phys. 29 (1990) 2052.
- [8] N. Nishimiya, T. Kishi, T. Mizushima, A. Matsumoto, K. Tsutsumi, J. Alloys Compd. 319 (2001) 312.
- [9] A. Pundt, C. Sachs, M. Winter, M.T. Reetz, D. Fritsch, R. Kirchheim, J. Alloys Compd. 293–295 (1999) 480.
- [10] A. Pundt, C. Sachs, M. Winter, M.T. Reetz, D. Fritsch, R. Kirchheim, Mater. Sci. Eng., B 108 (2004) 19.
- [11] S. Kishore, et al., J. Alloys Compd. 389 (2005) 234.
- [12] J. Haglund, F.F. Guillermet, G. Grimvall, M. Korling, Phys. Rev., B 48 (1993) 11685.
- [13] J. Waser, H.A. Levy, S.W. Peterson, Acta Crystallogr. 6 (1953) 661.
- [14] A. Züttel, Mater. Today 6 (2003) 24.
- [15] E. Wicke, H. Brodowsky, in: G. Alefeld, J. Vökle (Eds.), Hydrogen in Metals II, Springer, 1978, 81 pp.
- [16] Y. Fukai, Z. Phys. Chem. 164 (1989) 165.
- [17] G.R. Pearson, Chem. Rev. 85 (1985) 41.
- [18] S. Nagasaka, J. Phys. Soc. Jpn., 50(1981) 1570 and ibid 52(1982) 898.
- [19] S. Emura, S. Gonda, Y. Matsui, H. Hayashi, Phys. Rev., B. 38 (1988) 3280.
- [20] S. Emura, K. Shirai, Y. Kubozono, Phys. Scr. T115 (2005) 507.